



Thermal Effect on Positive Patterned Self-Assembled Monolayer Grown from a Droplet of Alkanethiol

Arindam Sannyal,^[a,b] Joonkyung Jang ^[b], Md. Shajahan,^[a] and Joyanta K. Saha ^{*[a]}

Atomic force microscope technique is widely used for the spatial narrow deposition of molecules inside the bare space of preexisting self-assembled monolayer (SAM) matrix. Using molecular dynamics simulation, we studied the formation of positively patterned SAM from a globule of 1-octadecanethiol (ODT) on predesigned SAM matrix of 1-dodecanethiol (DDT) and effect of temperature on it. The alkyl chains of ODT SAM were densely packed and ordered by means of chemisorption through sulfur atoms. The circular SAM of ODT contained defects due to the molecules those were standing upside down or trapped inside ODT SAM. We found that with the increase of temperature, these defects moved out by flipping of inverted ODT molecules or building spaces to be adsorbed on Au

surface. The ODT molecules on the top of the pile of stable circular SAM or those are upside down and trapped disperse in a unique fashion namely serial pushing through which molecules firstly make a free space to enter inside the adsorbed thiol molecules and then push neighboring molecules to get enough space to be adsorbed on the gold surface. The stability of ODT SAM was confirmed by analyzing different structural properties such as tilt angle, tilt orientation, and backbone orientation. We also calculated the diffusion coefficient of the ODT molecules which were on the top of SAM island. © 2019 Wiley Periodicals, Inc.

DOI: 10.1002/jcc.26042

Introduction

The well-defined growth, structure, and ease preparation of self-assembled monolayers (SAMs) have put them in the forefront for customizing the interfacial properties of metal and semiconductor surfaces. Fabrication of nanometer-scale patterns on surfaces has been widely carried out with specified size and geometry where an atomic force microscopy (AFM) tip can selectively displace some resistive molecules by the sequential adsorption of new adsorbates. As the formation, structure, and control of SAMs are nowadays well established, SAMs have begun to be patterned^[1] by using a wide range of scanning probe lithographic techniques such as microcontact printing,^[1,2] nanoimprinting, dip-pen lithography (DPN) in nanografting,^[1] nanopen reader and writer (NPRW),^[3] and photolithography.^[2] AFM technique containing a solution of adsorbate causes them to eject as a droplet in real-time experiments. By intensifying the local interactions, that is, the tip–SAM interactions of AFM and scanning tunneling microscope, SAMs can be patterned more sharply.^[3] Regarding this, positive patterning of SAMs,^[1,4] where adsorbates from preexisting bulk SAM matrix are removed and longer chain adsorbate molecules are grafted, is widely used to delineate transistors and other electronic components, in micro-electromechanical systems, optics, and electrical sensors.^[5]

Xu et al. studied different scanning probe microscope (SPM) and scanning probe lithography-based nanografting to evaluate the stability of the patterned SAM.^[4] Reed et al. observed the subsequent chemisorptions of conjugated oligomers onto the patterned sites in a SPM lithography technique by applying voltage pulses for the in situ replacement of 1-dodecanethiol (DDT) SAM.^[6] Theoretical study of orientation, conformation,

and the phase separation reproduced the experimental observation for a mixed SAM composed of short- and long-chain alkanethiols,^[7–10] whereas the latter ones form a denser crystalline-like assembly on spherical gold nanoparticles.^[11,12] Saha et al. revealed that the SAM island grown from a droplet of 1-octadecanethiol (ODT) resembled the bulk SAM in terms of stability and order, but it incorporates defects where the molecules were in an overturned position on the surface.^[13] The subjects regarding the range of formation of these structures, the thermal stability, nature of the defects, etc., are still unsettled. It is indeed very important to know the formation mechanism of positive patterned SAM, the influence of long-chain adsorbate on the properties of short-chain SAM matrix and the mechanism of removal of defects during formation of positive-patterned SAM by heat treatment.

Herein by the molecular dynamics (MD) simulation, we investigated the dynamic and static behavior of both bulk and SAM island. We considered DDT as preexisting bulk SAM matrix and a droplet of ODT as circular SAM island to be positively patterned on the gold surface. When an ODT droplet was brought into contact of a bulk SAM of DDT then the molecules of bulk SAM were repelled by the ODT adsorbates. Thus, this successive repellent is possible depending on the chain length, degree of order, and topography of the gold surface leading to a stable

[a] A. Sannyal, Md. Shajahan, J. K. Saha
Department of Chemistry, Jagannath University, Dhaka-1100, Bangladesh
E-mail: joys643@chem.jnu.ac.bd

[b] A. Sannyal, J. Jang
Department of Nanoenergy Engineering, Pusan National University, Busan
46241, Republic of Korea

Contract Grant sponsor: Jagannath University Research Fund

© 2019 Wiley Periodicals, Inc.

SAM through the intermolecular interactions between molecules in the SAM.^[2] Since SAMs were formed by spontaneous adsorption of adsorbate molecules, it is natural to find some defects in SAMs due to both intrinsic and extrinsic reasons.

Simulation Methods

We simulated a globular droplet of ODT on a gold (111) surface relevant to the experimental DPN, where the periodic slab boundary condition was considered.^[14–16] The relaxed gold surface of two layers containing a total of 6728 atoms was fixed in its position. First, we covered the surface by adsorbing DDT and then made a hole of a 40 Å diameter of the DDT SAMs. Then, a droplet of 245 ODT molecules was allowed to form SAM at the hole from a height of 2.0 nm of the surface. United atoms (UAs)^[10,12] model was taken account for the CH₃, CH₂, and SH groups of both DDT and ODT which corresponds to the simulation with all-atom models.^[17,18] As H atoms were accounted implicitly, current coarse graining was minimal. In MD simulation, the motion of particles was given by

$$F_i = m_i \frac{d^2 r_i}{dt^2} \quad (1)$$

Here, m_i is the mass of the particle and r_i is the particle's spatial position. The potential energy was calculated by using

$$F_i = -\nabla_i V \quad (2)$$

Harmonic potentials were used to describe the interactions between UAs such as bond stretching and bending angle.^[19] Triple cosine function of the dihedral angle φ was specified to maintain minima to the corresponding *trans* and *gauche* conformations of the four-atom torsion potential (C–C–C–C or C–C–C–S), respectively.^[20] Lennard-Jones (LJ) potentials were taken for the nonbonded interactions.

$$V_{LJ}(r) = 4\epsilon \left[\left(\frac{\sigma}{r_{ij}} \right)^{12} - \left(\frac{\sigma}{r_{ij}} \right)^6 \right] \quad (3)$$

where r is the interatomic distance, ϵ and σ are the LJ energy and length parameters, respectively.^[10] Lorentz-Berthelot combination rules^[21] were followed for the LJ framework of the heteroatomic pairs. The chemisorption interaction between S–Au pair was modeled by a Morse potential.^[22]

$$V_{Au-S}(r) = D_e \exp[-\alpha(r-r_e)] \{ \exp[-\alpha(r-r_e)] - 2 \} \quad (4)$$

where r is the interatomic distance of the S–Au atom pair, and D_e and r_e are the well-depth and the distance at the minimum

Table 1. Lennard-Jones (LJ) and Morse potential parameters for the UAs.

LJ	σ (Å)	ϵ (kcal/mol)	α
SH	4.25	0.397	-
CH ₂	3.905	0.118	-
CH ₃	3.905	0.175	-
Morse			
Au-S	2.65	8.763	1.47

of the potential energy, respectively. The LJ and Morse parameters those have been used in our simulation^[10,23,24] are shown in Table 1.

The MD simulations were carried out in DLPOLY-2.20 package^[25] at the constant number, volume, and temperature of 300 K (NVT ensemble) using the Berendsen thermostat.^[26] The velocity Verlet algorithm of 1.0 fs timescale was used for numerical integration of the equation of motion. The spherical droplet of 245 ODT molecules was equilibrated through an NVT simulation at 300 K for 2 ns which was then placed 2.0 nm above the surface. For the dispersion and evolution of the droplet resulting in the circular SAM pattern, a 40-ns-long MD trajectory was simulated without any external force. The resulting patterned SAM was then heated to 390 K with an increment of 10 K. At each temperature, an NVT MD simulation was run for 10 ns using the DLPOLY-2.20^[25] package as described above.

Several structural properties such as tilt angle θ_i , tilt orientation \vec{v}_i (Fig. 1), sulfur–sulfur distance (d_{ss}), and chain conformations of the ODT adsorbates were investigated at room temperature and compared with those of bulk DDT SAM matrix. For each molecule i , we defined its tilt direction in terms of a vector \vec{u}_i (Fig. 1).^[10,27] The polar angle \vec{u}_i relative to the surface normal of the i th molecule is attributed for the tilt angle θ_i . The order parameter of the molecular orientation was given by^[28]

$$O_u = \left\langle 0.5 \left[3 \left(\vec{u}_i \cdot \vec{u}_j \right)^2 - 1 \right] \right\rangle_{i \neq j} \quad (5)$$

where $\langle \rangle_{i \neq j}$ is the average over all the intermolecular pairs.

Diffusion coefficient (D) was calculated at room temperature for the ODT molecules which were on the top of the ODT SAM pile after the 40 ns, to evaluate their diffusion extent with time. The time-dependent diffusion coefficient was derived from mean square displacement (MSD) versus time traces.^[29] Specifically, the ensemble MSD was calculated using the evolution of particle displacement $[x(t), y(t), z(t)]$ ^[29] as a function of each time interval (Δt) according to:

$$\text{MSD}(n\Delta t) = \frac{\sum_{m=1}^{N-n} [x(m\Delta t + n\Delta t) - x(m\Delta t)]^2 + [y(m\Delta t + n\Delta t) - y(m\Delta t)]^2 + [z(m\Delta t + n\Delta t) - z(m\Delta t)]^2}{N-n} \quad (6)$$

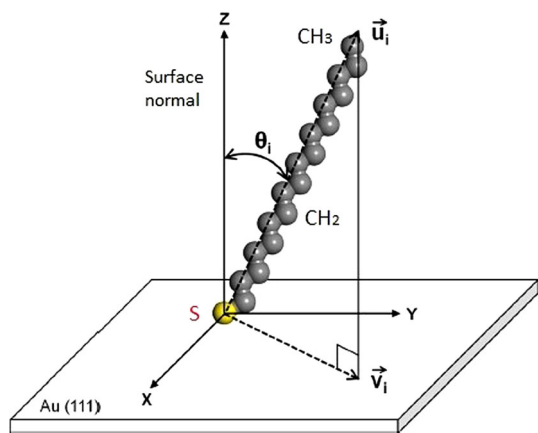


Figure 1. Schematic diagram of the molecular orientation of UAs of 1-octadecanethiol (ODT) with all-*trans* conformations on Au (111). For each molecule i , the tilt direction vector \vec{u}_i was defined by selecting UAs of CH₃ or CH₂ groups, which have odd (1–17) numbers of intervening CH₂ groups between them and the S atom. \vec{u}_i was defined as the average of the direction vectors from the S atom to these selected UAs, whereas \vec{v}_i is defined as the surface (XY plane) projection of \vec{u}_i . The tilt angle θ_i is the polar angle of \vec{u}_i measured from the surface normal (Z direction). [Color figure can be viewed at wileyonlinelibrary.com]

where N is the total number of time samples and $N-n$ is the number of interval samples per $n\Delta t$. Subsequently, the time-dependent diffusion coefficient $D(\Delta t)$ was estimated using:

$$D(n\Delta t) = \frac{\text{MSD}(n\Delta t)}{6n\Delta t} \quad (7)$$

Results and Discussion

The ODT molecules of the droplet (Fig. 2a) was triggered by van der Waals force to the surface resulting in a hemispherical shape (Fig. 2b, at 280 ps) which further flattened out due to the molecular twisting. Due to the adsorption of ODT molecules on the surface, the alkyl chains got organized and packed together (Fig. 2c, at 5 ns). We found that majority (70%) of the total 245 ODT molecules of the droplet rapidly got adsorbed on the gold surface within 10 ns. Duly, an ordered SAM island formed along with a heap on top of it (Fig. 2d), where further adsorption took place with increasing time. At a long time ($t > 10$ ns), relevant to an experimental timescale for the growth of SAMs in DPN lithography,^[30–32] there were a tiny droplet of 24 ODT molecules (9% of total), remaining on top of the pile of the SAM island. Noticeably, among these 24 ODT molecules, 11 ODT molecules got adsorb on the surface by a distinct pathway named serial pushing. In serial pushing mechanism (Fig. 3), the numbered molecules sitting on top of the ODT SAM island push the molecules below away, perforate down, and eventually adsorb to the surface.^[13] Another distinct mechanism, namely hopping down, was accounted by Saha et al. for the adsorption of ODT molecules on the bare surface. In the hopping-down process, the molecules diffuse on top of the SAM island reach to the edge of the SAMs island and slid down to the surface.^[13] But, at room temperature, we

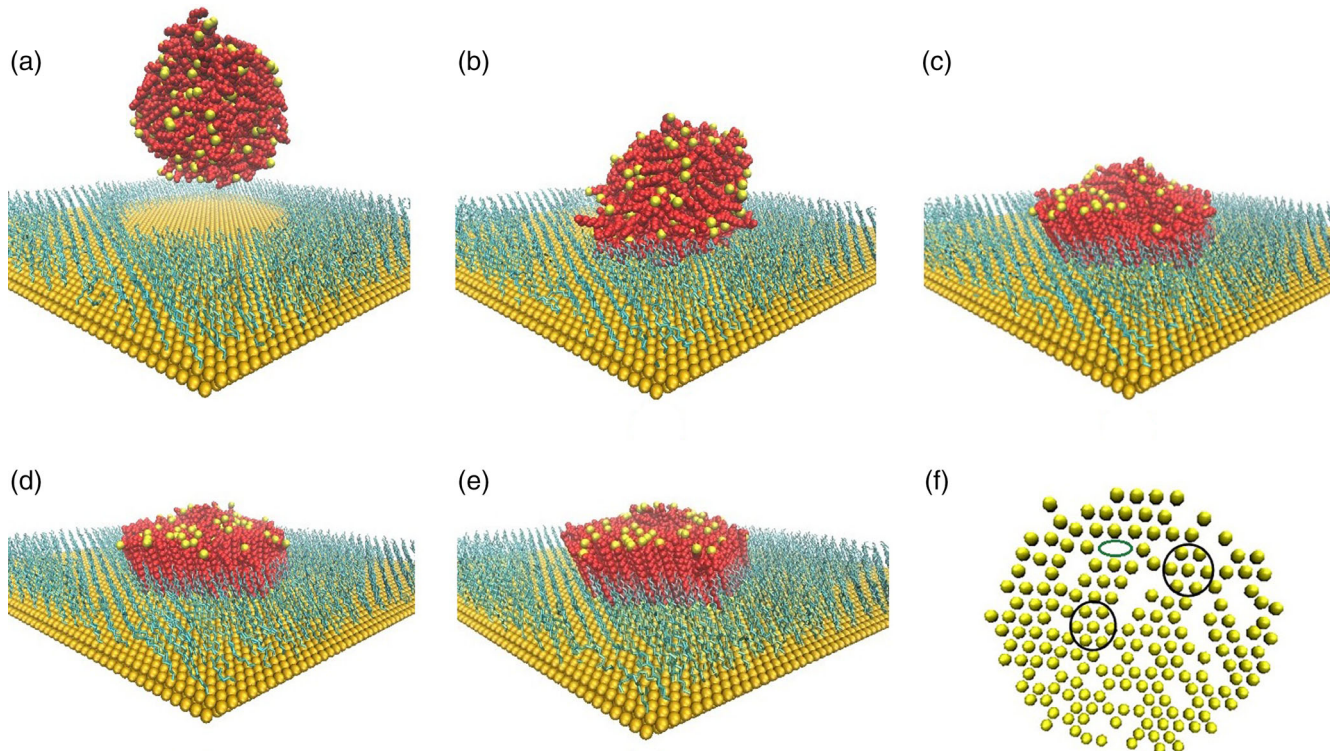


Figure 2. Positive-patterned SAM has grown from a droplet of 245 ODT molecules, scattering on Au (111) surface. a) Primary configuration droplet 2 nm above the surface; b) hemispherical shape of the ODT droplet after 280 ps; c) and d) were snapshots at 5 and 10 ns, respectively; e) ordered and packed SAM island after 40 ns; and f) S atoms with $(\sqrt{3} \times \sqrt{3})R30^\circ$ overlayer structure (black circle), whereas the vacant sites (green oval) are regarded as defects in SAM. For visual clarification, the DDT SAM matrix (cyan) and ODT SAM droplet (red) were taken in different colors and modes. [Color figure can be viewed at wileyonlinelibrary.com]

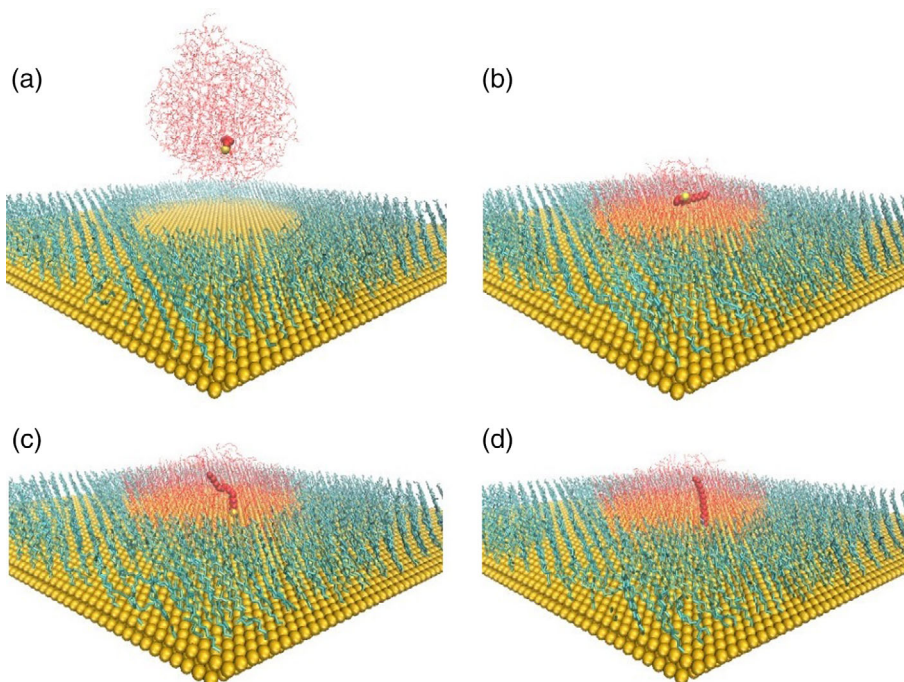


Figure 3. Four snapshots illustrate the serial pushing mechanism of the ODT molecule that where the ODT and DDT molecules are in different colors and modes for visual clarity. a) Initially, the ODT molecule was in the droplet; b) snapshot was taken at 10 ns where the molecule was on the top of the pile; c) at $t > 10$ ns, the molecule pushed the molecules those were below it to get space; and d) at 11.78 ns, the molecule got adsorbed on the surface. [Color figure can be viewed at wileyonlinelibrary.com]

did not observe such mechanism due to the presence of bulk DDT SAM matrix which restricted this adsorption pathway by causing unavailable space and hindrance. At 20 ns, the circular SAM island became more ordered (Fig. 2e) and finally a bulk-like SAM island was formed (Fig. 2f, at 40 ns) but somewhat tilted away from the surface normal. Most of the sulfur atoms developed a $(\sqrt{3} \times \sqrt{3})R30^\circ$ overlayer.^[13,33] Mostly, the S atom of an ODT molecule was closer to the surface than its CH_3 tail (upright state), whereas in some ODT molecules the CH_3 — group was found to be closer the surface than the S atom (inverted state). We assigned discrete spin value for the orientation of each molecule to study the ordering process of the upright and inverted ODT molecules (+1 spin and -1 spin, respectively). It is regarded that in the inverted position, an ODT molecule gets anchored by the CH_3 tail with the surface and cannot get out from this state because the molecule is trapped by the neighboring molecules through the interchain van der Waals force.^[13] We found that at room temperature, 48 ODT molecules got anchored at the Au (111) surface with the CH_3 group instead of S atom at the end of 40 ns. Besides, at room temperature, 10 out of the total 245 ODT molecules remained unbound after 40 ns and trapped in between the neighboring ODT molecules by the interchain packing. These trapped ODT molecules did not adsorb on the surface either by the CH_3 — group or by the S atom. In addition, two ODT molecules were in the stripped phase,^[33] that is, they were lying down on the surface (Fig. S4a).

Initially, when the ODT molecules were in a droplet at 2 nm above from the surface, the percentage of the inverted molecules was almost 100% due to random orientation. The percentage decreased sharply and approached 20% within 10 ns and finally converged to 19.6% at 40 ns (Fig. 4a). This implies that in the ODT SAM, the molecules were predominantly in upright. The percentage fluctuation after 10 ns is due to the flipping of the ODT molecules which were remained on the top of the pile of the SAM

island. On excluding the ODT molecules of the small pile, the percentage of the inverted molecules converged to 19.2% after 35 ns without any fluctuations. The inverted ODT molecules result in the imperfection of SAM island. Usually, defects are found in SAMs due to vacancies or disordered molecules.^[34] Although X-ray photoelectron spectroscopy showed the presence of unbound thiolate molecules in SAM,^[35,36] currently it is not specific enough whether those unbound thiols were inverted as mentioned above or due to the molecules on top of the SAM or contributed by both. Any thermal swelling may cause flipping of the inverted ODTs, thus

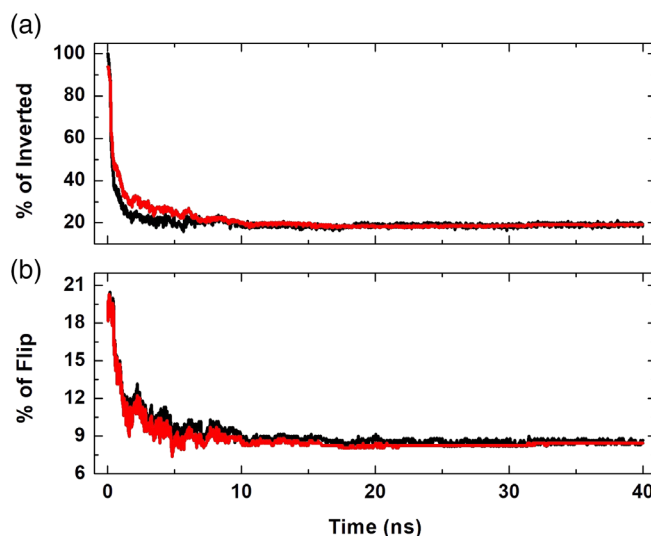


Figure 4. Percentage of a) the inverted ODT molecules and b) flipped ODT molecules as a function of time. The red lines show the percentages of inverted and flipping molecules excluding the molecules belonging to the small pile on top of the SAM island. [Color figure can be viewed at wileyonlinelibrary.com]

removing defects in the SAM island and causing all the S atoms to bind to the surface.^[13] We accounted that after few picoseconds, a certain number of ODT molecules got desorbed from surface, that is, from their initial inverted state and then again got adsorbed by their individual S atoms, leads to the upright phase. These molecules are regarded as flipped molecules as the phenomena resemble flipping. Any configurational change from the inverted state (-1 spin) to the upright state ($+1$ spin) was considered as the flipping.^[13] We checked the number of flipped molecules at a given time. As the droplet spread, the flipping percentage decreased from $\sim 18\%$ and converged to 8.5% after 30 ns (Fig. 4b). If the molecules of the small pile on top of the ODT island are excluded, the percentage of the flipped molecules leveled off to 8.2% without any fluctuations. Even at the end of 40 ns, the percentage of flipping was about 8.5% . This might be because some of the ODT molecules still remained unbound to the surface. At room temperature, the unbound molecules did not get enough space in order to get adsorbed. None of the upright and inverted molecules could flip at room temperature, because their S atoms fastened to the surface and trapped by neighboring molecules via interchain packing, respectively.

In addition, after 40 ns, 3 of 245 ODT molecules were found to be on top of the SAM island. As they were not bound either by the S atom or the CH_3 tail group with the surface, not even trapped in SAM, they continued to diffuse on the pile of the circular SAM island. We calculated the diffusion coefficient of these three ODT molecules by MSD (eq. 7). MSD was calculated as the evolution of displacement of the molecules as a function of each time interval

(eq. 6). The MSD was calculated in terms of finite displacement within 30 – 40 ns as initially all of the ODT molecules were detached from the surface and at $t > 20$ ns, an ordered SAM had formed. We considered the linear fitting to determine the diffusion coefficient (D) from the slope of MSD (Fig. S1). The calculated diffusion coefficient was $40416.7 \text{ nm}^2 \text{ s}^{-1}$. Sheehan and Whitman experimentally reported that the surface diffusion coefficient of ODT on pristine gold surface was $8400 \pm 2300 \text{ nm}^2 \text{ s}^{-1}$.^[37] The diffusion of the present ODT molecules is higher because they were at the top of the ODT SAM, whereas in the experimental study the ODT molecules were adsorbed to the bare gold surface by means of covalent-type bond.

We evaluated several structural features such as percentage of *trans* conformation, tilt angle, tilt direction, and backbone orientation for both circular ODT and bulk DDT SAM to contemplate how the positive patterned ODT SAM affected the bulk one. In order to verify the parameters with the bulk ODT SAM, we only considered the molecules anchored by the S atoms with the surface. To assess the percentage of *trans* and *gauche* conformations with time, dihedral angles of alkane chains of both DDT and ODT were calculated. The mean distance of the neighboring S–S pairs (d_{SS}) in the ODT circular SAM decreased from an initial value of 5.85 \AA and converged to 4.67 \AA at 40 ns (Fig. 5a₁), which is greater than the bulk SAM value of 4.50 \AA .^[38] The d_{SS} of the DDT bulk molecules fractionally increased from an initial value of 4.66 \AA to a final value of 4.68 \AA (Fig. 5a₂) at the end of 40 ns. This is because the adsorbed ODT molecules implied pressure to the immediate DDT molecules which in turn suppressed their neighboring molecules and

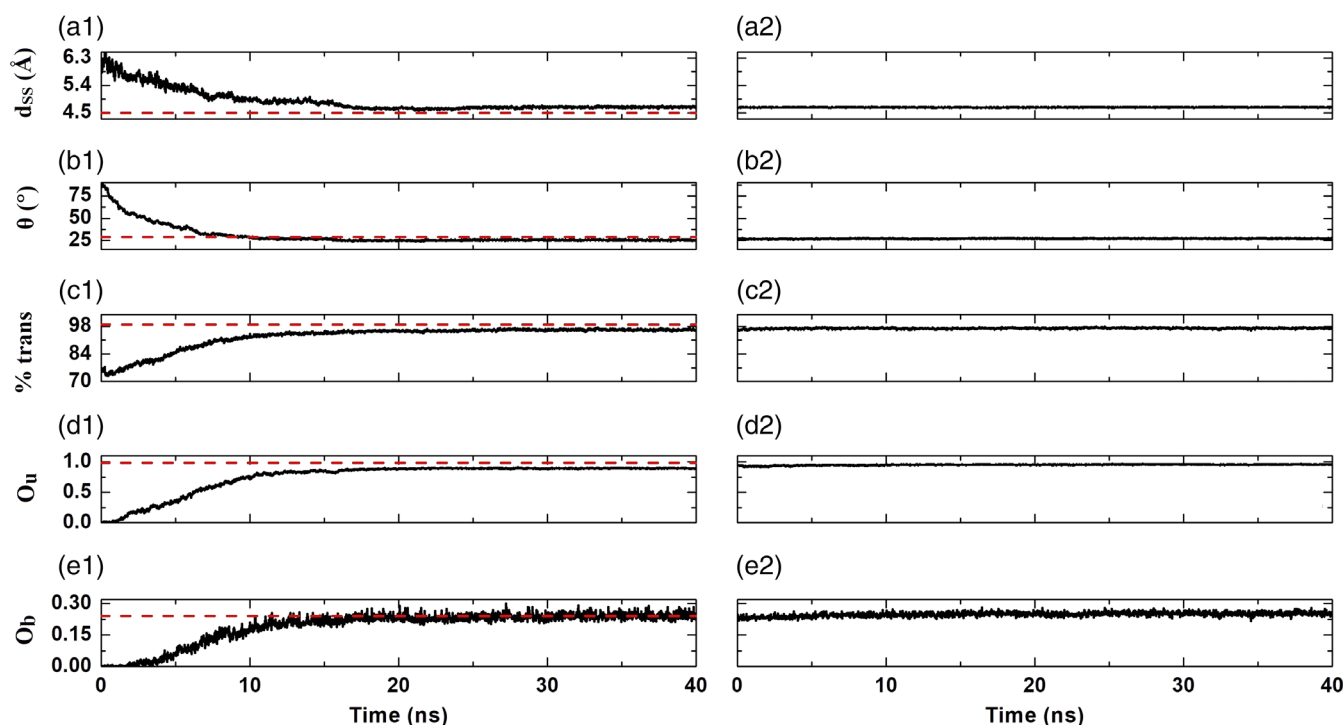


Figure 5. Variation of structural parameters of ODT droplet (left) and bulk DDT (right) with time. a) Neighboring sulfur–sulfur distance d_{SS} ; b) tilt angle θ ; c) percentage of *trans* conformations; d) order parameter of the tilt direction O_u ; and e) backbone orientation O_b of alkyl chains. The red broken lines show the corresponding values of the bulk ODT SAM. [Color figure can be viewed at wileyonlinelibrary.com]

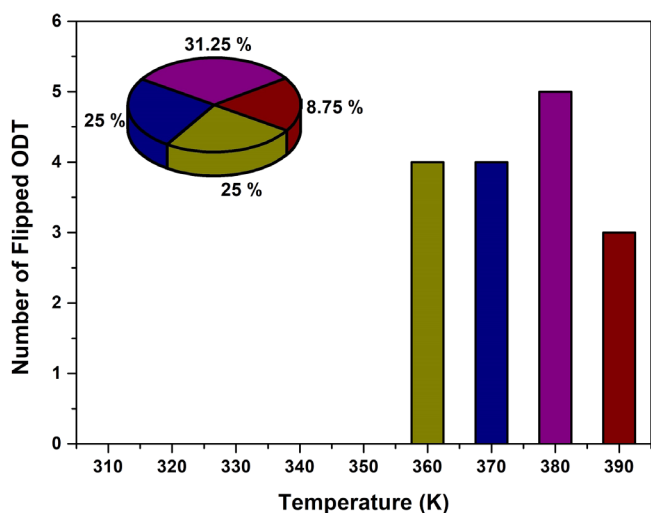


Figure 6. Number of flipped ODT molecules from the inverted state at different temperatures. The inset pie chart shows the percentage of the 16 flipped ODT molecules at elevated temperatures. [Color figure can be viewed at wileyonlinelibrary.com]

continued to the periphery. In general, each molecule tilted away from the surface normal by about $\sim 30^\circ$ in a stable and ordered SAM.^[33,39] The tilt angle of the alkyl chains (θ) of ODT molecules decreased rapidly with time from 0 to 10 ns and then slowly to a plateau at 15 ns and finally converged to 25.6° (Fig. 5b₁) at 40 ns, which is slightly lower than the bulk ODT SAM (29°) because of compaction by DDT bulk SAM.^[13] Whereas, for the DDT SAM molecules, θ increased from an initial value of 26.75° to 27.25° (Fig. 5b₂) because of lateral pushing by the ODT molecules. Initially, the percentage of *trans* conformations of ODT molecules was 75% as the molecules were in random conformations in the droplet, however, converged to 96% at 40 ns (Fig. 5c₁) which may increase further with the longer timescale. It is marginally lower than the bulk value of 99%,^[38] evidential that the SAM formed from the droplet of ODT molecules was a stable one. On the other hand, the percentage of the *trans* conformation of DDT molecules was initially about 96% and then converged to 97% at 40 ns (Fig. 5c₂) due to the influence of ODT SAM island. As the majority of the molecules were adsorbed to the surface within 10 ns, the tilt direction (O_u) of the ODT molecules increased sharply and converged to 0.89 (Fig. 5d₁) at 40 ns, which is lower than that of the bulk ODT SAM ($O_u = 0.98$).^[38] The DDT SAM has an almost ideal alignment of 0.96 at 40 ns (Fig. 5d₂). The backbone orientation (O_b) for ODT molecules followed the O_u trends to 10 ns and then converged to 0.24 (Fig. 5e₁), which is close to the bulk value of 0.24.^[38] The O_b of the bulk DDT SAM had increased from an initial value of 0.248 to 0.25 (Fig. 5e₂).

We studied the thermal effect on the inverted and trapped ODT molecules inside the ODT SAM. We found that among 48 inverted ODT molecules, 16 ODT molecules flipped with raising the temperature up to 390 K. Figure 6 represents the number of flipped ODT molecules with increasing temperature and Figure S2 shows the mechanism of flipping of an ODT molecule at 360 K. In addition, in the temperature range of 330–350 K, three inverted ODT molecules desorbed from the surface,

diffused to the bulk DDT SAM, and then followed the serial pushing to be adsorbed in the bulk DDT SAM (Fig. S3) and formed a nano-sized island. On the other hand, in the temperature range of 310–330 K, 5 out of the 10 trapped ODT molecules adsorbed on the surface in the ODT circular SAM. Whereas, five ODT molecules diffused to bulk DDT SAM matrix and then followed the serial pushing to be adsorbed in the bulk DDT SAM. Finally, after rising temperature up to 370 K, two new tiny nano-sized ODT SAM islands formed by five and three ODT molecules (Fig. S3).

We further evaluated the progress of the three ODT molecules that were diffusing on top of SAM pile at 300 K. Among them, two ODT molecules adsorbed in the circular ODT SAM region at 310–320 K and one in the bulk DDT SAM at 330 K. At room temperature, the diffusion kinetics of these three ODT molecules were not high enough to get adsorbed on the surface, however, at higher temperature these ODT molecules got enough kinetic energy to be adsorbed in the circular and bulk SAM. In addition, the two stripped ODT molecules (at 300 K) become ordered at elevated temperature. As shown in Figure S4a–c, one stripped ODT molecule sequentially stands to the upright position at 320 K. Whereas, the other ODT molecule becomes bent at 330 K and then ordered at 360 K (Fig. S4d–f).

Conclusion

Using MD simulation, we studied the formation, the nature of the defects, and thermal effect on those defects in the system consisting DDT as bulk SAM matrix and a droplet of ODT as an adsorbate on Au (111) surface. We found that a stable SAM of ODT molecule was formed within 10 ns, where the majority (70%) of the ODT molecules adsorbed by the S atom leading to an ordered, packed, and a $(\sqrt{3} \times \sqrt{3}) R30^\circ$ overlayer structure. A distinct pathway was found named serial pushing for the adsorption of the remaining ODT molecules those were on top of the pile of SAM at $t > 10$ ns, whereas no hopping-down mechanism was found at room temperature. A certain portion of the ODT molecules were found of which the CH_3 tail groups were closer to the surface than the corresponding S atom—referred as inverted one leading to the imperfections in the positive patterned SAM island. The SAM formed by the ODT molecules had the bulk-like structural features but moderately differ in *trans* conformation, tilt angle, and tilt direction. On the other hand, the structural properties of the DDT matrix insignificantly changed from the initial values due to the circular SAM formed by the ODT molecules. The ODT SAM become more defect free with increasing temperature, because no ODT molecules were on top of the pile or stacked in between other ODT molecules. Elementary controlling and modeling of positive patterned SAM from direct-write lithography are believed to accumulate from the insight of this dynamic study.

Acknowledgment


The author acknowledges the support of Jagannath University Research Fund for this study.

Conflict of Interest

The authors declare no competing financial interest.

Keywords: self-assembled monolayer · alkanethiol · positive pattern · MD simulation · defect

How to cite this article: A. Sanyal, J. Jang, M. Shajahan, J. K. Saha. *J. Comput. Chem* **2019**, *40*, 2636–2642. DOI: 10.1002/jcc.26042

 Additional Supporting Information may be found in the online version of this article.

- [1] R. K. Smith, P. A. Lewis, P. S. Weiss, *Prog. Surf. Sci.* **2004**, *75*, 1.
- [2] J. C. Love, L. A. Estroff, J. K. Kriebel, R. G. Nuzzo, G. M. Whitesides, *Chem. Rev.* **2005**, *105*, 1103.
- [3] G. Yang, N. A. Amro, G.-Y. Liu, *Proc. SPIE* **2003**, *5220*, 52.
- [4] S. Xu, S. Miller, P. E. Laibinis, G.-Y. Liu, *Langmuir* **1999**, *15*, 7244.
- [5] S. K. Arya, P. R. Solanki, M. Datta, B. D. Malhotra, *Biosens. Bioelectron.* **2009**, *24*, 2810.
- [6] J. Chen, M. A. Reed, C. L. Asplund, A. M. Cassell, M. L. Myrick, A. M. Rawlett, J. M. Tour, P. G. V. Patten, *Appl. Phys. Lett.* **1999**, *76*, 624.
- [7] S. J. Stranick, A. N. Parikh, Y.-T. Tao, D. L. Allara, P. S. Weiss, *J. Phys. Chem.* **1994**, *98*, 7636.
- [8] S. Chen, L. Li, C. L. Boozer, S. Jiang, *Langmuir* **2000**, *16*, 9287.
- [9] J. I. S. I. R. McDonald, *Thin Films* **1998**, *24*, 205.
- [10] J. Hautman, M. L. Klein, *J. Chem. Phys.* **1989**, *91*, 4994.
- [11] W. D. Luedtke, U. Landman, *J. Phys. Chem. B* **1998**, *102*, 6566.
- [12] P. K. Ghorai, S. C. Glotzer, *J. Phys. Chem. C* **2007**, *111*, 15857.
- [13] H. Kim, J. K. Saha, Z. Zhang, J. Jang, M. A. Matin, J. Jang, *J. Phys. Chem. C* **2014**, *118*, 11149.
- [14] C. A. Mirkin, S. Hong, L. Demers, *Chem. Phys. Chem.* **2001**, *2*, 37.
- [15] S. Hong, C. A. Mirkin, *Science* **2000**, *288*, 1808.
- [16] D. S. Ginger, H. Zhang, C. A. Mirkin, *Angew. Chem. Int. Ed.* **2004**, *43*, 30.
- [17] W. Mar, M. L. Klein, *Langmuir* **1994**, *10*, 188.
- [18] J. P. Bareman, M. L. Klein, *J. Phys. Chem. C* **1990**, *94*, 5202.
- [19] W. L. Jorgensen, D. S. Maxwell, J. Tirado-Rives, *J. Am. Chem. Soc.* **1996**, *118*, 11225.
- [20] W. L. Jorgensen, J. D. Madura, C. J. Swenson, *J. Am. Chem. Soc.* **1984**, *106*, 6638.
- [21] M. P. Allen, D. J. Tildesley, *Computer Simulation of Liquids*, Oxford University Press, New York, **1987**.
- [22] X. Zhao, Y. Leng, P. T. Cummings, *Langmuir* **2006**, *22*, 4116.
- [23] J. K. Saha, Y. Ahn, H. Kim, G. C. Schatz, J. Jang, *J. Phys. Chem. C* **2011**, *115*, 13193.
- [24] Y. Ahn, J. K. Saha, G. C. Schatz, J. Jang, *J. Phys. Chem. C* **2011**, *115*, 10668.
- [25] W. Smith, C. W. Yong, P. M. Rodger, *Mol. Simul.* **2002**, *28*, 385.
- [26] H. J. C. Berendsen, J. P. M. Postma, W. F. v. Gunsteren, A. DiNola, J. R. Haak, *J. Chem. Phys.* **1984**, *81*, 3684.
- [27] R. Bhatia, B. J. Garrison, *Langmuir* **1997**, *13*, 4038.
- [28] S. Fujiwara, T. Sato, *J. Chem. Phys.* **1999**, *110*, 9757.
- [29] J. D. Fowlkes, C. P. Collier, *Lab Chip* **2013**, *13*, 877.
- [30] J. Jang, S. Hong, G. C. Schatz, M. A. Ratner, *J. Chem. Phys.* **2001**, *115*, 2721.
- [31] H. Kim, J. Jang, *J. Phys. Chem. A* **2009**, *113*, 4313.
- [32] H. Kim, G. C. Schatz, J. Jang, *J. Phys. Chem. C* **2010**, *114*, 1922.
- [33] F. Schreiber, *Prog. Surf. Sci.* **2000**, *65*, 151.
- [34] C. Vericat, M. E. Vela, R. C. Salvarezza, *Phys. Chem. Chem. Phys.* **2005**, *7*, 3258.
- [35] B. Singhana, S. Rittikulsittichai, T. R. Lee, *Langmuir* **2012**, *29*, 561.
- [36] S. D. Techane, L. J. Gamble, D. G. Castner, *Biointerphases* **2011**, *6*, 98.
- [37] P. E. Sheehan, L. J. Whitman, *Phys. Rev. Lett.* **2002**, *8*, 156104.
- [38] J. K. Saha, H. Kim, J. Jang, *J. Phys. Chem. C* **2012**, *116*, 25928.
- [39] W. GM, K. JK, L. JC, *Sci. Prog.* **2005**, *88*, 17.

Received: 31 May 2019

Revised: 19 July 2019

Accepted: 23 July 2019

Published online on 14 August 2019